haematologica
Journal of the Ferrata Storti Foundation

SQSTM1::RARA fusion in acute promyelocytic leukemia: the first case report and literature review

by Xiaomei Yin, Na Li; Zhanrui Cheng, Jia Ai, Hong Liang, Shu Sun and Hong-Hu Zhu

Received: December 4, 2025.
Accepted: April 10, 2026.

Citation: Xiaomei Yin, Na Li; Zhanrui Cheng, Jia Ai, Hong Liang, Shu Sun and Hong-Hu Zhu. SQSTM1::RARA fusion in acute promyelocytic leukemia: the first case report and literature review. Haematologica. 2026 Apr 23. doi: 10.3324/haematol.2025.300329 [Epub ahead of print]

SQSTM1::RARA fusion in acute promyelocytic leukemia: the first case report and literature review

Xiaomei Yin[1]*, Na Li [2, 3]*, Zhanrui Cheng[2, 3], Jia Ai[1], Hong Liang[1], Shu Sun[2, 3], Hong-Hu Zhu[2, 3]#

* These authors contributed equally to the research study.

1. Department of Hematology, Changchun Central Hospital, Changchun, China;
2. Department of Hematology, Beijing Chao-Yang Hospital, Capital Medical University, Beijing, China;
3. Institute for Cancer, Chinese Institutes for Medical Research (CIMR), Beijing, China

Funding: This work was supported by the National Natural Science Foundation of China (82450101, 82370169), the "Dengfeng" Talent Training Program of Beijing Hospitals Authority (DFL20240301), and the funds from the Chinese Institutes for Medical Research, Beijing (CIMR) to Hong-Hu Zhu.

Corresponding Author: Hong-Hu Zhu, PhD, MD

Address: Beijing Chao-Yang Hospital, 8 Gongren Tiyuchang Nanlu, Chaoyang District, Beijing, 100020; 10 Xitoutiao, Youanmen Wai, Fengtai District, Beijing 100069, China

E-mail: zhuhhdoc@163.com

Authors' Disclosures: The authors declare that they have no competing interests.

Authors' Contributions: Xiaomei Yin, Jia Ai, Hong Liang collected the clinical data. Na Li, Zhanrui Cheng, Shun Sun analyzed the genetic results. Hong-Hu Zhu and Na Li drafted the manuscript. All authors approved the final version.

Data Sharing Statement: All data generated or analyzed during this study are included in this published article.

Acute promyelocytic leukemia (APL) with typically *PML::RARA* fusion gene caused by t (15;17) (q24; q21) was distinguished from other types of acute myeloid leukemia[1]. However, a few cases that can not be identified with *PML::RARA* by using conventional methods involve abnormal promyelocytes that are fully in accordance with APL in morphology, cytochemistry, and immunophenotype[2 3]. In this report, we identified the *SQSTM1::RARA* and reciprocal *RARA::SQSTM1* fusions for the first time in a patient lacking t (15;17)(q24;q21)/*PML::RARA* fusion. Then, this patient proved resistant to induction therapy based on all-trans retinoic acid (ATRA). To date, a comprehensive literature review has identified 21 novel *RARA* fusion partner genes distinct from *PML::RARA*. The *SQSTM1::RARA* reported in our study represents the 22nd such fusion. Among these variant fusions, *ZBTB16::RARA, TTMV::RARA,* and *STAT5B::RARA* are the most frequently reported and are associated with clinical features that differ from those of *PML::RARA* positive APL.

The index case was an 82-year-old man initially admitted to a local hospital because of persistent fatigue for over 10 days (clinical course is summarized in Figure 1A). Blood tests showed white blood cell count of 0.66×10^9/L, and absolute neutrophil count of 0.07×10^9/L, hemoglobin level of 93 g/L, and platelet count of 93×10^9/L. Bone marrow examination revealed abnormal promyelocytes accounting for 88.5%. These cells were characterized by round nuclei and abundant small azurophilic granules, but no Auer rods were observed (Figure 1B). Flow cytometry (FCM) identified 85.8% myeloblasts with an immunophenotype positive for CD13, CD33, CD45, CD117, CD64, and MPO, while negative for CD34, CD11b and HLA-DR. Notably, the absence of CD38 expression presented a distinctive feature compared to classic *PML::RARA*-positive APL (Figure 1C). The presumptive initial diagnosis of this patient was APL. However, both Reverse Transcription Polymerase Chain Reaction (RT-PCR) and Fluorescence In Situ Hybridization (FISH) using the standard *PML::RARA* dual-color dual-fusion probe failed to detect the classic *PML::RARA* fusion. Instead, FISH analysis revealed an atypical signal pattern in 71.5% of cells, characterized by three *RARA* signals (red) and two *PML* signals (green) (Figure 1D). In the context of the

karyotype findings, this pattern suggests that the t(5;17) breakpoint did not split the RARA locus. Instead, the intact RARA gene was translocated to the derivative chromosome 5. The presence of an extra derivative chromosome 5, as confirmed by karyotyping, accounts for the three RARA signals observed. The karyotype analysis confirmed: 46,X,-Y,t(5;17)(q35;q21),der(5)t(5;17),+8[2]/46,idem,r(1),add(12)(p13)[14]/46,XY[4] (Figure 1E). Whole Transcriptome Sequencing (WTS) was subsequently performed, revealing a novel *SQSTM1::RARA* fusion gene involving *SQSTM1* (5q35) and *RARA* (17q21). The fusion results from the joining of exon 5 of *SQSTM1* to exon 3 of *RARA*. Bioinformatic analysis of the sequencing data confirmed that this fusion is in-frame and is predicted to generate a functional chimeric protein. The reciprocal *RARA::SQSTM1* fusion was also detected (Figure 2A). WTS analysis revealed downregulated *CD38* transcript levels and upregulated *BCL2* transcript levels (Figure 2B). These findings may explain the absence of surface protein detection by FCM and the marked sensitivity to subsequent venetoclax (VEN) therapy. Furthermore, comparative transcriptomic analysis between our patient, classical APL patients, and non-APL AML patients identified numerous differentially expressed genes. Enrichment analysis demonstrated that, compared to classical APL and non-APL AML patients, our patient exhibited upregulation of multiple pathways related to protein translation (Figure 2C). We subsequently validated this result using PCR and Sanger sequencing (Figure 2D&E). Additionally, next-generation sequencing mutation analysis revealed *TET2* and *BRCA2* mutations. *TET2* p.Y592Lfs*46 was detected at a variant allele frequency (VAF) of 41.0%, and this mutation induces premature translational termination, generating a truncated protein. *BRCA2* p.P512R missense mutation was found with a VAF of 46.5%.

Given the high clinical suspicion of APL, the patient promptly initiated dual induction therapy. The specific regimen included arsenic trioxide (ATO) at 0.15 mg/kg daily (administered as 10 mg/day) and all-trans retinoic acid (ATRA) at 25 mg/m² daily (administered as 20 mg twice daily). The patient's body mass index was 23.4 kg/m² . Steroid prophylaxis was not administered during the induction phase. However, ATO

and ATRA were discontinued on day 5 due to a negative *PML::RARA* fusion gene result and a poor early response showing no signs of differentiation. A follow-up BM examination 33 days after induction chemotherapy showed a predominance of promyelocytes (88%) with 1% myeloblasts, and myeloperoxidase staining was strongly positive. The patient was then started on a regimen of VEN (100 mg orally on day 1) and azacitidine (100 mg subcutaneously). On the first day of dosing, the patient developed dyspnea and decreased oxygen saturation and was transferred to the ICU. Two weeks later, a repeat BM aspirate showed 84.5% of promyelocytes. The patient subsequently began a 9-day combination therapy of VEN and ATRA. The VEN dose was escalated as follows: 50 mg daily (days 1–3), 100 mg daily (days 4–5), and 200 mg daily (days 6–9). Concomitant ATRA was maintained at 20 mg twice daily throughout this period (days 1–9). During treatment, the patient experienced adverse events—including fever, dyspnea, pleural effusion, and renal dysfunction—which prompted the concurrent administration of intravenous dexamethasone (5 mg daily from day 1 to day 7). On day 10, the patient refused to continue oral VEN and ATRA therapy. Management was subsequently limited to supportive care only. Forty-three days after discontinuation of therapy, blood test at our institution revealed a white blood cell count of 10.36×10^9/L, hemoglobin of 86 g/L, and platelet count of 253×10^9/L. BM morphology examination showed only 1% promyelocytes. Most notably, minimal residual disease (MRD) by FCM was negative. The patient was subsequently transferred to the Urology Department for a minimally invasive procedure to address benign prostatic hyperplasia. The patient presented to our hospital for a follow-up visit one year later and BM smear showed relapse. RNA sequencing of the BM aspirate detected the *SQSTM1::RARA* and the reciprocal *RARA::SQSTM1* fusions, with exon breakpoints identical to those identified at the initial diagnosis. This finding confirms the role of *SQSTM1::RARA* as the driver gene in this case.

The human *SQSTM1* gene, located on chromosome 5, spans approximately 16 kilobases and consists of eight exons [4 5]. It encodes the multifunctional p62/SQSTM1 protein, which is primarily recognized as a selective autophagy receptor that targets

cellular components for lysosomal degradation [6]. Beyond its role in autophagy, p62 functions as a pivotal signaling hub due to its capacity to interact with diverse partners. It critically regulates key pathways including Nrf2-mediated oxidative stress response[7], mTORC1-dependent nutrient sensing[8], and NF-κB-driven inflammation[9]. Notably, p62 dysregulation is implicated in tumorigenesis; gene copy gains in the 5q locus are linked to clear cell renal cell carcinoma, partly through p62 overexpression[10], and p62 accumulation is a common feature observed in numerous cancer types[7 11 12].

This case presents a unique therapeutic trajectory that offers insights into venetoclax biology. The patient showed clear resistance to conventional ATRA/ATO therapy, consistent with the absence of *PML::RARA* rearrangement. However, the rapid development of dyspnea, hypoxemia, and renal dysfunction within 24 hours of a single 100 mg venetoclax dose—in combination with azacitidine—strongly suggests incipient tumor lysis syndrome, providing compelling in vivo evidence of exceptional venetoclax sensitivity. Despite this early toxicity, subsequent treatment with low-dose venetoclax (escalated to 200 mg) combined with ATRA for only nine days was sufficient to induce deep remission. Most remarkably, forty-three days after all therapy was discontinued, bone marrow examination revealed only 1% promyelocytes with negative minimal residual disease by FCM. This durable response following limited treatment exposure suggests that even brief BCL-2 inhibition may trigger sustained leukemic clearance in genetically susceptible subsets. We hypothesize that the novel genetic abnormality identified in this case may confer profound BCL-2 dependence, rendering the clone exquisitely sensitive to venetoclax despite resistance to standard APL-directed therapy. The concurrent *TET2* and *BRCA2* pathogenic variants may provide additional context for this patient's atypical course. *TET2* mutations are associated with clonal hematopoiesis and enhanced sensitivity to hypomethylating agents like azacitidine, which the patient received. The *BRCA2* variant, involving the homologous recombination repair pathway, may contribute to genomic instability and facilitate accumulation of multiple genetic lesions. Together, these variants highlight the value of comprehensive genomic profiling in understanding complex treatment responses.

Unlike the classic *PML::RARA* fusion, which is highly sensitive to ATRA and ATO, most rare *X::RARA* variants are known to confer resistance to standard differentiation therapy. Clinical management of these resistant cases remains challenging; however, current literature suggests potential benefits from intensive chemotherapy or novel targeted agents. Notably, BCL-2 inhibitors such as VEN and the antibody-drug conjugate gemtuzumab ozogamicin (GO) have emerged as promising salvage therapies. Beyond therapeutic responses, distinct clinicopathological features have been observed in specific variants. *TTMV::RARA* cases show a higher incidence in juveniles (<18 years: 75.8%), while *FIP1L1::RARA* occurs primarily in young children (≤3 years: 62.5%) with a female predominance (75%). Additionally, all reported *BCOR::RARA* cases were male and exhibited loss of the Y chromosome. From a diagnostic perspective, WTS is instrumental in discovering novel fusions. For rare fusions like *SQSTM1::RARA* that show suboptimal responses, early molecular identification and transition to alternative potent therapies are crucial for improving outcomes. The characteristics of the 22 *X::RARA* cases are summarized in Table 1.

Ethical review and approval were not required for this case report in accordance with local legislation and institutional requirements. The study was conducted in accordance with the ethical standards of the People's Republic of China. Written informed consent was obtained from the patient for publication of this case report and accompanying images.

References

1. Grimwade D, Biondi A, Mozziconacci MJ, et al. Characterization of acute promyelocytic leukemia cases lacking the classic t(15;17): results of the European Working Party. Groupe Français de Cytogénétique Hématologique, Groupe de Français d'Hematologie Cellulaire, UK Cancer Cytogenetics Group and BIOMED 1 European Community-Concerted Action "Molecular Cytogenetic Diagnosis in Haematological Malignancies". Blood. 2000;96(4):1297-1308.
2. Wen L, Xu Y, Yao L, et al. Clinical and molecular features of acute promyelocytic leukemia with variant retinoid acid receptor fusions. Haematologica. 2019;104(5):e195-e199.
3. Guarnera L, Ottone T, Fabiani E, et al. Atypical rearrangements in APL-like acute myeloid leukemias: molecular characterization and prognosis. Front Oncol. 2022;12:871590.
4. Jeong SJ, Zhang X, Rodriguez-Velez A, Evans TD, Razani B. p62/SQSTM1 and selective autophagy in cardiometabolic diseases. Antioxid Redox Signal. 2019;31(6):458-471.
5. Kumar AV, Mills J, Lapierre LR. Selective autophagy receptor p62/SQSTM1, a pivotal player in stress and aging. Front Cell Dev Biol. 2022;10:793328.
6. Lee DH, Park JS, Lee YS, et al. SQSTM1/p62 activates NFE2L2/NRF2 via ULK1-mediated autophagic KEAP1 degradation and protects mouse liver from lipotoxicity. Autophagy. 2020;16(11):1949-1973.
7. Shi Q, Jin X, Zhang P, et al. SPOP mutations promote p62/SQSTM1-dependent autophagy and Nrf2 activation in prostate cancer. Cell Death Differ. 2022;29(6):1228-1239.
8. Liu K, Qiu D, Liang X, et al. Lipotoxicity-induced STING1 activation stimulates MTORC1 and restricts hepatic lipophagy. Autophagy. 2022;18(4):860-876.
9. Zhong Z, Umemura A, Sanchez-Lopez E, et al. NF-κB restricts inflammasome activation via elimination of damaged mitochondria. Cell. 2016;164(5):896-910.
10. Li L, Shen C, Nakamura E, et al. SQSTM1 is a pathogenic target of 5q copy number gains in kidney cancer. Cancer Cell. 2013;24(6):738-750.
11. Mondal G, Gonzalez H, Marsh T, et al. Autophagy-targeted NBR1-p62/SQSTM1 complexes promote breast cancer metastasis by sequestering ITCH. Nat Cell Biol. 2025;27(7):1098-1113.
12. Sánchez-Martín P, Saito T, Komatsu M. p62/SQSTM1: 'Jack of all trades' in health and cancer. FEBS J. 2019;286(1):8-23.

Table 1. Characteristics of 22 *X::RARA* Fusions

X::RARA	N	Age (Median)	Gender (n/N, %)	Cytogenetic	Sensitive Regimens (n/N, %)	Detection Method (n/N, %)	Common Mutations (n/N, %)
ZBTB16::RARA	39	7-83(53)	M(28,71.8%) F(10,25.6%) 1 unknown	t(11;17)(q23;q12)	□ATRA+Chemo(6,15.4%) □Chemo(5,12.8%) □VEN+DAC(1,2.6%) □GO+DA(1,2.6%) □VEN(1,2.6%) □ATRA+ATO(1,2.6%) □IDA+ATO(1,2.6%)	RT-PCR(20,51.3%) WTS(3,7.7%) Southern blot□1,2.6%)	*TET2(5,12.8%)* *ARID1A(5,12.8%)* *IDH2(3,7.7%)* *SRSF2(3,7.7%)* *CEBPA(3,7.7%)* *FLT3(3,7.7%)* *RUNX1(2,5.1%)* *CSF3R(2,5.1%)* *NRAS(1,2.6%)* *SMARCA4(1,2.6%)* *KDM6A(1,2.6%)* *SAMD9(1,2.6%)* *ZRSR2(1,2.6%)* *KMT2C(1,2.6%)*
TTMV::RARA	33	2-49(8) (<18ys: 25,75.8%)	M(19,57.6%) F(14,42.4%)	--	□ATRA+Chemo(8,24.2%) □ATRA+ATO(4,12.1%) □Chemo(3,9.1%) □ATRA;ATO (or ATRA)+VEN(2,6.1%) □ATRA;ATO (or ATRA)+ VEN+Chemo(2,6.1%) □VEN+AZA(1,3.0%)	WTS(33,100%)	*NRAS(4,12.1%)* *FLT3(3,9.1%)* *WT1(2,6.1%)* *ARID1B(1,3.0%)* *SAMD9(1,3.0%)* *TCF3(1,3.0%)* *ARID1A(1,3.0%)* *KMT2C(1,3.0%)* *DHX15(1,3.0%)* *KRAS(1,3.0%)* *BRAF(1,3.0%)* *DNMT3A(1,3.0%)*
STAT5b::RARA	19	17-67(41)	M(16,84.2%) F(3,15.8%)	der(17)	□Chemo(8,42.1%) □ATRA;ATO(or ATRA)+ Chemo(4,21.1%) □VENE+Chemo(2,10.5%) □ATRA(1,5.3%) □GO(1,5.3%)	RT-PCR(14,73.7%) WTS(3,15.8%) 5'-RACE(1,5.3%)	*RARA(1,5.3%)* *STAT5b(1,5.3%)*
NPM1::RARA	13	0.5-74(12)	M(9,69.2%) F(4,30.8%)	t(5;17)(q35;q12)	□ATRA;ATO(or ATRA)+ Chemo(10,77.0%) □Chemo(2,15.4%) □ATRA(1,7.7%) □ATO alone or ATO-based therapy(1,7.7%)	RT-PCR(8,61.5%) Southern blot(1,7.7%)	--
IRF2BP2::RARA	8	19-76 (48.5)	M(4,50%) F(4,50%)	t(1;17)(q42;q21)	□ATRA;ATO(or ATRA alone)+Chemo(3,37.5%) □ATRA+ATO+GO(1,12.5%) □ATRA(1,12.5%) □GO(1,12.5%)	WTS(6,75%) RT-PCR(1,12.5%) 5'-RACE(1,12.5%)	*WT1(2,25%)* *FLT3(1,12.5%)* *NRAS(1,12.5%)* *PHF6(1,12.5%)* *KIT(1,12.5%)* *ARID1B(1,12.5%)*
FIP1L1::RARA	8	0.75-90(2.65) (≤3ys:5,62.5%)	F(6,75%) M(2,25%)	t(4;17) (q12;q21)	□ATRA;ATO(or ATRA)+ Chemo(3,37.5%) □ATRA(1,12.5%) □Chemo(1,12.5%)	WTS(2,25%) RT-PCR(2,25%) 5'-RACE(2,25%) Conventional karyotype analysis(1,12.5%)	*KRAS(1,14.3%)* *NRAS(1,14.3%)* *MAP2K2(1,14.3%)N F1(1,14.3%)* *FLT3(1,14.3%)*
TNRC18::RARA	4	50-61(58.5)	M(3,75%) F(1,25%)	t(7;17) (p22; q21)	□ATRA+VEN(1,25%) □VEN+ATRA+AZA(1,25%) □VEN+AZA(1,25%) □ATRA+IDA+Ara-C(1,25%)	WTS(3,75%) FISH(1,25%)	*TET2(1,25%)* *WT1(1,25%)* *ATG2B(1,25%)*
TBL1XR1::RARA	4	--	--	t(3;17)(q26;q21)	□ATO+MTZ(1,25%) □Chemo(1,25%)	WTS(1,25%) 5'-RACE(1,25%)	--
BCOR::RARA	3	45-71(47)	M(3,100%)	t(X;17)(p11;q21) and all cases showed -Y	□ATRA alone or ATRA-based therapy(2,66.7%) □IDA+Ara-C(1,33.3%)	WTS(2,66.7%) 5'-RACE(1,33%)	*NRAS(1,33.3%)* *KRAS(1,33.3%)* *FLT3(1,33.3%)*
STAT3::RARA	3	24-45(26)	M(2,66.7%) F(1,33%)	t(17;17) (q21;q12)	--	WTS(3,100%)	--
TFG::RARA	3	16-56(56)	F(2,66.7%) M(1,33.3%)	t(3;14;17) (q12;q11;q21)	□VEN+ATRA(2,66.7%) □ATRA(1,33.3%)	WTS(2,66.7%) Targeted RNA-seq(1,33.3%)	*SBDS(1,33.3%)*
PRKAR1A::RARA	2	66-67(66.5)	F(1,50%) M(1,50%)	t(17;17)(q24;q12)	ATRA;ATO(or ATRA)+ Chemo(2,100%)	WTS(1,50%)	*KRAS(1,50%)*
NUP98::RARA	2	31-70(50.5)	M(2,100%)	t(11;17) (p15;q21)	IDA+Ara-C(1,50%)	WTS(2,100%)	--
HNRNPC::RARA	2	29-41(35)	M(1,50%) F(1,50%)	t(14;17)(q11;q21)	VEN+AZA(1,50%)	WTS(2,100%)	*PHF6(1,50%)*
IRF2BP1::RARA	1	51	F	t(19;17)(q13;q21)	Sensitive to ATRA	WTS	--
THRAP3::RARA	1	34	M	t(1;17) (q3;q21)	VEN+DAC	WTS	--
NuMA::RARA	1	0.5	M	t(11;17)(q13;q21)	Sensitive to ATRA	--	--
FNDC3B::RARA	1	36	M	t(1;17)(q42;q21)	Ara-C+DNR	5'-RACE	--
OBFC2A::RARA	1	59	M	t(2;17)(q32;q21)	ATRA+IDA+Ara-C	Array CGH analysis	--
NAB2::RARA	1	73	M	t(12;17) (q13;q21)	--	WTS	*TET2;ZRSR2; SRSF2;IDH2*
GTF2I::RARA	1	35	M	t(7;17)(q11;q21)	--	5'-RACE	--
SQSTM1::RARA	1	82	M	t(5;17)(q35;q21)		WTS	*TET2;BRCA2*

Chemo: Chemotherapy; DAC: Decitabine; GO: Gemtuzumab Ozogamicin; DA:Daunorubicin and Cytarabine; IDA: Idarubicin; AZA: Azacitidine; 5'RACE: 5'-Rapid Amplification of CDNA Ends; Ara-C: Cytarabine; MTZ: Mitoxantrone; N: Total reported number of cases for each fusion subtype, data are presented as n/N (%)

Figure 1. Clinical, morphological, immunophenotypic, and cytogenetic features of the index case at diagnosis. A. Clinical course of the patient. B. High-power view of the bone marrow aspirate smear at initial diagnosis (Wright-Giemsa stain). The leukemic cells exhibit round nuclei and abundant small azurophilic granules, consistent with hypergranular promyelocytes. Note the absence of Auer rods. C. FCM analysis of the BM aspirate at initial diagnosis. Representative scatter plots show the distinct clustering of the abnormal cell population (highlighted in red), distinguishable from internal normal lymphocytes (green population) and erythroblasts (gray population). Standard quadrant or boundary gates demarcate positive and negative populations, with thresholds defined by internal controls. D. FISH analysis of bone marrow cells using a *PML* (15q24, green) / *RARA* (17q21.1, red) dual-color, dual-fusion probe. Left panel: A normal control interphase nucleus exhibiting the expected wild-type pattern of two *PML* and two *RARA* signals (2G2R). Right panel: A representative interphase nucleus from the patient exhibiting an atypical signal pattern consisting of two *PML* signals and three *RARA* signals (2G3R). E. G-banded karyotype of the BM aspirate at initial diagnosis. A complex abnormal karyotype was identified: 46,X,-Y,t(5;17)(q35;q21),der(5)t(5;17),+8[2]/46,idem,r(1),add(12)(p13)[14]/46,XY[4].

Figure 2. Molecular and transcriptomic characterization of *SQSTM1::RARA* and reciprocal *RARA::SQSTM1* fusions. A. Schematic representation of the SQSTM1::RARA and the reciprocal *RARA::SQSTM1* fusions detected by WTS in BM aspirate smear at initial diagnosis and relapse. B. Median *BCL2* expression (log2(TPM+1)) in our patient, TCGA Classical APL (n=14), TCGA Non-APL-AML (n=137), and a GTEx healthy control group (n=372). C. Volcano plots of differentially expressed genes in our patient versus classical APL (top left) and non-APL AML (bottom left). Bar charts of upregulated pathways versus classical APL (top right) and non-APL AML (bottom right). D. Detection of the partial *SQSTM1::RARA* (left, 615 bp) and *RARA::SQSTM1* (right, 629 bp) fusions transcripts in cDNA. The specific primer sequences used were: SQSTM1::RARA: 5'-CTTGTGTAGCGTCTGCGAGGGAAAG-3' (Forward) and 5'-CGGTCGTTTCTCACAGACTCCTTGG-3' (Reverse); RARA::SQSTM1: 5'-CATGGCCAGCAACAGCAGCTC-3' (Forward) and 5'-GCATCTGGGAGAGGGACTCAATCAG-3' (Reverse). E. Sanger sequencing validation of *SQSTM1*-exon

5 fused to *RARA*-exon 3 (left), and the reciprocal *RARA*-exon 2 fused to *SQSTM1*-exon 6 (right) in BM aspirate at initial diagnosis.

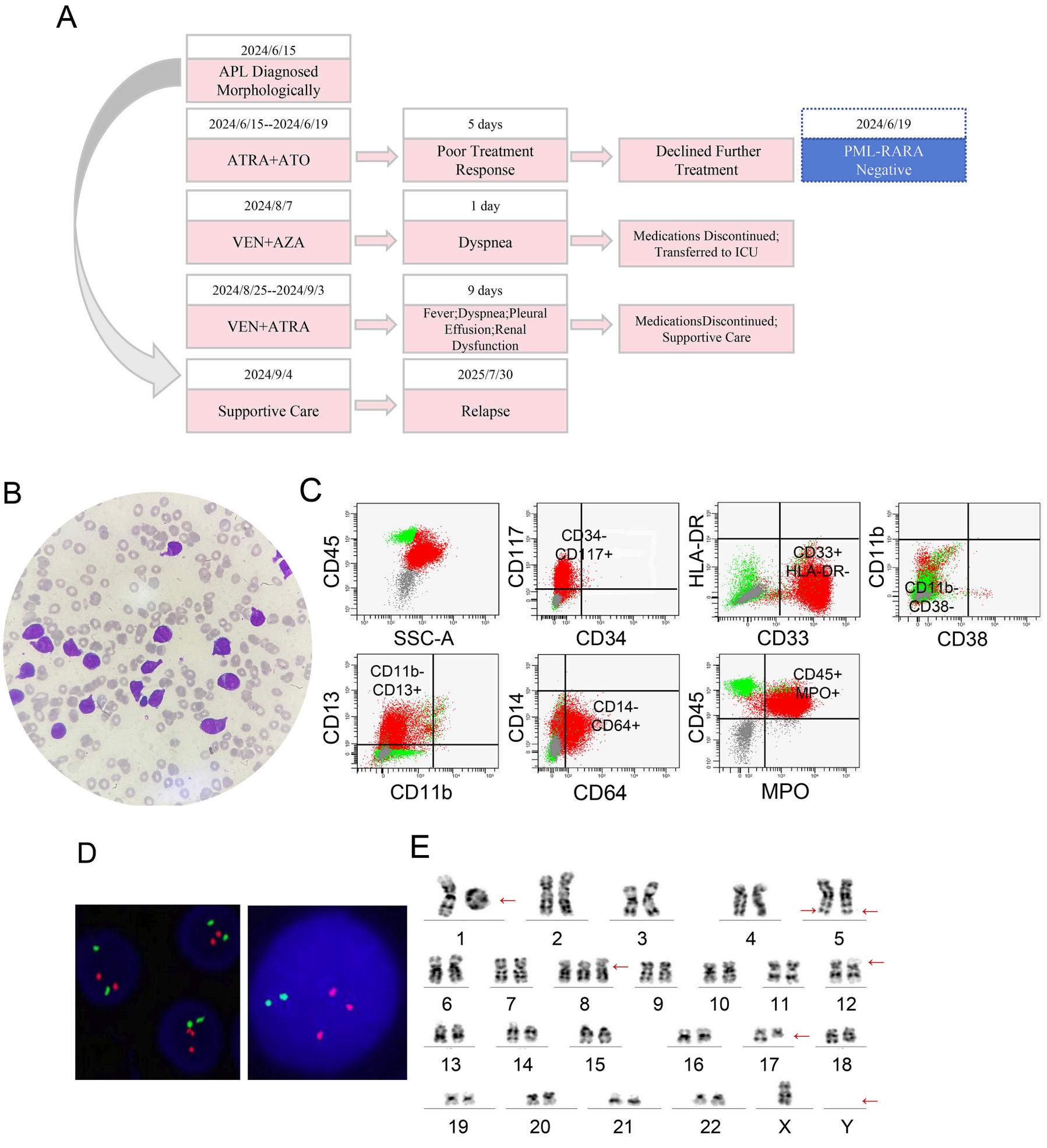
A
2024/6/15
APL Diagnosed Morphologically
2024/6/15--2024/6/19
ATRA+ATO
5 days
Poor Treatment Response
Declined Further Treatment
2024/6/19
PML-RARA Negative
2024/8/7
VEN+AZA
1 day
Dyspnea
Medications Discontinued; Transferred to ICU
2024/8/25--2024/9/3
VEN+ATRA
9 days
Fever;Dyspnea;Pleural Effusion;Renal Dysfunction
MedicationsDiscontinued; Supportive Care
2024/9/4
Supportive Care
2025/7/30
Relapse
B
C
CD45
SSC-A
CD117
CD34
CD34-
CD117+
HLA-DR
CD33
CD33+
HLA-DR-
CD11b
CD38
CD11b-
CD38-
CD13
CD11b
CD11b-
CD13+
CD14
CD64
CD14-
CD64+
CD45
MPO
CD45+
MPO+
D
E
1
2
3
4
5
6
7
8
9
10
11
12
13
14
15
16
17
18
19
20
21
22
X
Y

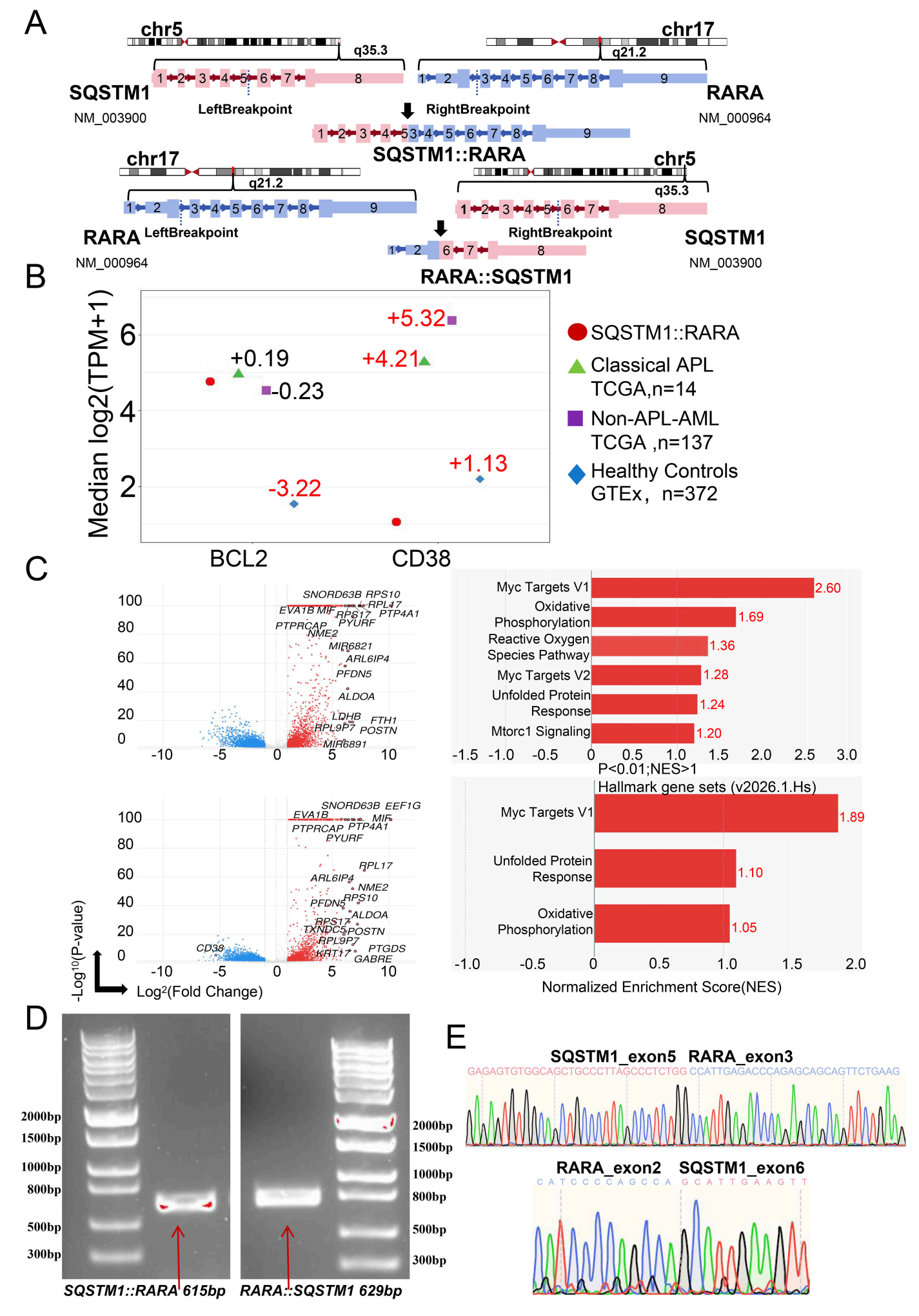
A
chr5
q35.3
chr17
q21.2
SQSTM1
NM_003900
LeftBreakpoint
RightBreakpoint
RARA
NM_000964
SQSTM1::RARA
chr17
q21.2
chr5
q35.3
RARA
NM_000964
LeftBreakpoint
RightBreakpoint
SQSTM1
NM_003900
RARA::SQSTM1
B
Median log2(TPM+1)
+5.32
+0.19
+4.21
-0.23
+1.13
-3.22
BCL2
CD38
SQSTM1::RARA
Classical APL TCGA,n=14
Non-APL-AML TCGA ,n=137
Healthy Controls GTEx, n=372
C
SNORD63B RPS10 RPL17 EVA1B MIF RPS17 PTP4A1 PTPRCAP PYURF NME2 MIR6821 ARL6IP4 PFDN5 ALDOA LDHB FTH1 RPL9P7 POSTN MIR6891
Myc Targets V1 2.60
Oxidative Phosphorylation 1.69
Reactive Oxygen Species Pathway 1.36
Myc Targets V2 1.28
Unfolded Protein Response 1.24
Mtorc1 Signaling 1.20
P<0.01;NES>1
SNORD63B EEF1G EVA1B MIF PTPRCAP PTP4A1 PYURF RPL17 ARL6IP4 NME2 RPS10 PFDN5 ALDOA RPS17 TXNDC5 POSTN RPL9P7 CD38 KRT17 PTGDS GABRE
Hallmark gene sets (v2026.1.Hs)
Myc Targets V1 1.89
Unfolded Protein Response 1.10
Oxidative Phosphorylation 1.05
-Log10(P-value)
Log2(Fold Change)
Normalized Enrichment Score(NES)
D
2000bp
1500bp
1000bp
800bp
500bp
300bp
SQSTM1::RARA 615bp
RARA::SQSTM1 629bp
E
SQSTM1_exon5 RARA_exon3
GAGAGTGTGGCAGCTGCCCTTAGCCCTCTGG CCATTGAGACCCAGAGCAGCAGTTCTGAAG
RARA_exon2 SQSTM1_exon6
CATCCCCAGCCA GCATTGAAGTT